On the preferential occurrence of interplanetary shocks in July and November: Causes (solar wind annual dependence) and consequences (intense magnetic storms)

E. Echer and W. D. Gonzalez
Geofísica Espacial, Instituto Nacional de Pesquisas Espaciais, São José dos Campos, Brazil

B. T. Tsurutani
Jet Propulsion Laboratory, California Institute of Technology, Pasadena, California, USA

L. E. A. Vieira, M. V. Alves, and A. L. C. Gonzalez
Geofísica Espacial, Instituto Nacional de Pesquisas Espaciais, São José dos Campos, Brazil

Received 5 April 2004; revised 15 October 2004; accepted 23 November 2004; published 2 February 2005.

[1] An annual dependence of interplanetary shock rate near 1 AU was found with preferential shock occurrence in July and in November. Although a solar origin for this dependence can not be discarded, it is shown that at least part of this shock distribution can be explained or caused by the annual dependence of solar wind parameters. Such annual dependence in plasma and magnetic field parameters makes the shock formation easier, in the second half year, due to the lower average solar wind bulk and characteristic speeds (Alfvenic and magnetosonic). These asymmetric interplanetary space propagation conditions are probably due to the Earth being exposed to solar wind from different solar magnetic hemispheres in both half years. Furthermore, the peaks in shock distribution are coincident with the peaks in the very intense geomagnetic storms distribution found by *Clúa de Gonzalez et al.* [2001]. It is suggested that the irregularity in geomagnetic activity is associated with the shock rate annual dependence. These results might imply that solar wind emitted from the opposite solar magnetic hemispheres has slightly different properties.

Citation: Echer, E., W. D. Gonzalez, B. T. Tsurutani, L. E. A. Vieira, M. V. Alves, and A. L. C. Gonzalez (2005), On the preferential occurrence of interplanetary shocks in July and November: Causes (solar wind annual dependence) and consequences (intense magnetic storms), *J. Geophys. Res.*, *110*, A02101, doi:10.1029/2004JA010527.

1. Introduction

[2] Since solar wind was discovered, more than 40 years ago, several studies have confirmed the existence of periodicities on timescales of 27 days, the solar rotation period [*Neugebauer and Snyder*, 1965], and of the 11-year solar cycle [*Neugebauer*, 1975; *Gazis*, 1996] on solar wind parameter variations. Intermediate periodicities between these two extremes have been studied only more recently. *Bolton* [1990] reported a 1-year variation in solar wind proton density N_p and speed V_{sw} close to Earth's orbit, which he attributed to an internal oscillation in the Sun or to the cometary's mass injection in the solar wind. Later, *Richardson et al.* [1994] and *Gazis et al.* [1995], from observations varying from ~0.72 to ~42 AU using several spacecrafts, found a 1.3-year period in solar wind variation whose origin was attributed to a possible oscillation in the Sun. However, the authors also comment that the explanation could be more complex. More recently, *Zieger and Mursula* [1998] have found a very clear annual variation in the solar wind speed. During the solar minima years 1965–1966 and 1987–1988 a semiannual variation is observed, and in solar minima years 1975–1976 and 1994–1995 an annual variation (with maxima around the March equinox) is found. *Zieger and Mursula* [1998] also believed that this annual variation exists only in solar minimum; that is, it is absent during solar maximum conditions. This annual variation was attributed by those authors to the orbital Earth's motions in a solar wind emitted from asymmetric solar magnetic hemispheres. *Paularena et al.* [1997] and *Szabo et al.* [1996], using 20 years of IMP 8 data, verified the existence of an annual variation for solar wind proton density, solar wind proton temperature (T_p), and solar wind speed.

[3] A semiannual variation in V_{sw} is expected with maximum around equinoxes (epoch when the Earth reaches maximum heliographic latitudes), and it is the basis of the axial mechanism explaining the semiannual variation in geomagnetic activity [*Priester and Cattani*, 1962; *Russell and McPherron*, 1973]. However, V_{sw} asymmetries were observed long ago by *Hundhausen et al.* [1971] when studying Vela solar wind observations during 1965–1968. They noted that the average V_{sw} was faster above the

0148-0227/05/2004JA010527$09.00

heliographic equator (in September) than below it (around March). It was suggested by them that a higher value of transient solar activity in the northern solar hemisphere could be the cause of their observations. However, recent works seem to show that the asymmetry is a persistent feature of the heliosphere, and it is not directly related to the solar activity [*Zieger and Mursula*, 1998].

[4] The above mentioned studies have focused mainly on the solar wind parameters. Neither propagation conditions for shocks nor the consequences of this annual dependence on solar wind parameters to the Earth's magnetosphere were assessed. In this work, as a result of analyzing data from 1973 to 2000, an unexpected asymmetry in shock distribution near 1 AU is presented. The shock rate was found to be (on a statistics basis) higher in July and November, when Earth was at a heliographic latitude of ~3°N, closer to the crossing of the heliomagnetic equator (in June and December) and it was more pronounced in November than in July. This variation was more noticeable in the vicinity of the 1979 and 2000 solar maxima. A detailed analysis of solar wind and interplanetary magnetic field (IMF) parameters was performed. An annual variation that seems to be comparable with the shock rate was found in a wide range of solar wind and IMF parameters. Results show that the second half year presents more favorable propagation conditions for shocks, which could partially explain the observed asymmetry in shock rate. These conditions are lower solar wind bulk speeds and also lower characteristic speeds, both Alfvenic and magnetosonic, when compared to average values. It is also suggested that these peaks in the annual shock distribution are associated with the irregularity observed in the annual variation of very intense magnetic storms found by *Clúa de Gonzalez et al.* [2001, 2002] in *aa*, *Dst*, and *AE* indices.

2. Methodology of Analysis

[5] The list of 574 shocks used in this study contains shocks that occurred between 1973 and 2000, and it was constructed based on the literature [*Abraham-Shrauner and Yun*, 1976; *Borrini et al.*, 1982; *Cane*, 1985; *Sheeley et al.*, 1985; *Tsurutani and Lin*, 1985; *Volkmer and Neubauer*, 1985; *Richter et al.*, 1986; *Schwenn*, 1986; *Cane et al.*, 1987; *Marsden et al.*, 1987; *Mihalov et al.*, 1987; *Richardson and Cane*, 1993; *Gosling et al.*, 1990; *Woo and Schwenn*, 1991; *Bravo and Pérez-Enriquez*, 1994; *Bothmer and Schwenn*, 1998; *Bravo and Blanco-Cano*, 1998; *Watari and Detman*, 1998; *Blanco-Cano and Bravo*, 2001; International Solar Terrestrial Physics Solar Wind Catalog Candidate Events, available at http://pwg.gsfc.nasa.gov/scripts/SWCatalog.shtml]. The period prior to 1972 had sparser solar wind observations coverage, and shocks observed in this early period are not used in this work.

[6] Solar wind daily average data obtained through the OMNIweb database during 1973–2000 have been used in this work in order to calculate the monthly average solar wind parameters: magnetic field strength B, solar wind proton density N_p, solar wind speed V_{sw}, and solar wind proton temperature T_p. Alfvenic and magnetosonic solar wind velocities were calculated based on the solar wind parameter monthly averages.

[7] Distributions of shocks, solar wind parameters, and geomagnetic indices were analyzed in the entire 1973–2000 period and also during solar maximum and minimum periods, independently. Exception occurs for the *AE* index, which is used in the period 1973–1994, because after 1994, due to problems in Russian geomagnetic observatories, only provisional values are available. In order to obtain the geomagnetic index intensity distributions the same criteria adopted by *Clúa de Gonzalez et al.* [2001, 2002] has been used.

[8] Since the solar cycle descending phase is longer than the ascending phase, it was decided to use 3 years before the solar minimum, the minimum year, and 2 years after it, in order to characterize the solar activity minimum period. On the other hand, to characterize the solar activity maximum period, it was decided to use 2 years before the maximum, the year of maximum, and 3 years later. As a result of this decision, we considered as solar minimum epochs the following periods: 1973–1978 and 1993–1998. The years 1983–1988, considered solar minimum according to this choice, have not been used due to the scarcity of data. As for the solar maxima epochs the considered periods were 1977–1982 and 1998–2000. The years 1977, 1978, and 1998 have been considered as part of solar minimum as well as of solar maximum.

3. Results

3.1. Annual Variation in Shock Occurrence Near 1 AU

[9] Using the total number of shocks catalogued from the literature in the period 1973–2000, the shock rate monthly distribution percentage near Earth was determined, and it is presented in Figure 1 (top). These shocks were driven for both interplanetary coronal mass ejections (ICMEs) and corotating interaction regions (CIRs). The literature sources do not permit the classification of every shock with a CIR or an ICME driver, but it is well known that the greatest number of shocks at 1 AU is driven by ICMEs, especially during solar maximum period [*Schwenn*, 1986; *Berdichevsky et al.*, 2000; *Echer et al.*, 2004].

[10] The occurrence of shocks was expected to be the same every month; that is, 1/12 = 0.083, or that in each month, 8.3% of the total number of shocks of the year occurred. The expected uniform distribution, which approximately coincides with the average value of monthly occurrence of shocks, is shown as a solid line in Figure 1. The top and bottom dotted lines represent the average plus and minus one standard deviation, respectively. Most of the months have a relative number of shocks lower than or comparable to the average/uniform distribution, but July (10.4% of the total number of yearly shocks, slightly above the upper curve of one standard deviation) and November (13.9% of the total annual of shocks; the number of shocks is larger than the mean value plus two standard deviation) have a significantly enhanced shock rate. The second half year has a somewhat higher shock rate than the first half, the integrated shock occurrence being 45.5% in the first half of year and 54.4% in the second half.

[11] The shock distribution was also determined for solar maximum and minimum periods, independently. Shocks were grouped in solar minimum epochs 1973–1978 (169 shocks) and 1993–1998 (93 shocks) and in

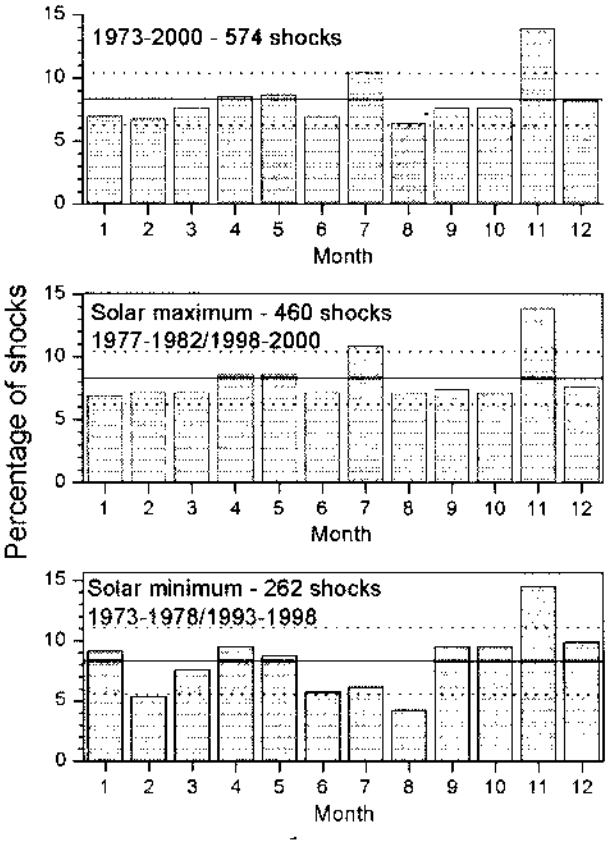

Figure 1. Monthly occurrence of interplanetary shocks near 1 AU. Percentages of shocks per month (top) in the period 1973–2000, (middle) around solar maximum periods, and (bottom) around solar minimum periods are shown. Average and one standard deviation of shock occurrence are indicated by the solid and dotted lines, respectively.

solar maximum epochs 1977–1982 (334 shocks) and 1998–2000 (126 shocks). As pointed out, due to the solar maximum and minimum epoch definition used, these data sets are not mutually exclusive; that is, there is a superposition of years in solar minimum and maximum epochs (1977–1978 and 1998 years are considered in both periods; neither of these years presents significant peaks in July or November). The number of shocks identified in the period 1983–1992 is very small due to the fact that solar wind measurements were sparse in that period. For this reason this period was not included in solar maximum and minimum averages. Figure 1 (middle) and Figure 1 (bottom) show the distribution of shocks calculated for solar maximum and solar minimum, respectively. It can be seen that during solar maximum the peaks in July and November are present, while during solar minimum, only the peak in November occurs. The occurrence of shocks in July is lower than in other months during solar minimum.

[12] A χ^2 test was applied to these distributions. The results do not permit the rejection of the null hypothesis of a uniform distribution at the 0.05 significance level. However, these results are not conclusive, because χ^2 values are high. For 11 degrees of freedom the $\chi^2_{0.95}$ value is 19.7, while the distribution values are solar minimum ($\chi^2 = 10.1$) and solar maximum ($\chi^2 = 5.7$); entire period ($\chi^2 = 5.65$). As the peak in November is well above one standard deviation, a real physical cause may be suspected. Furthermore, this distribution has a sporadic character, which means it is not present every year. Figure 2 shows the monthly variation of interplanetary shocks occurrence near 1 AU for successive years for half of one solar cycle: 1995, 1996, 1997, 1998, 1999, and 2000. Years are marked on the left, and the total number of shocks is on the right. The distribution average is indicated by the solid line, while the dotted lines represent average plus and minus one standard deviation. It is seen that individual years can have distributions very different from the total/whole data set. In the examples shown in Figure 2 it is noticed that July peak occurs in 1996 and 2000. Although it is not shown, the July peak was also observed in 1975, 1980, 1982, and 1996 years. Similarly, November peak is more important during some years (1997, 2000, and also in 1975, 1977 (comparable to the September peak), and 1980). During other years the July and November peaks are absent or are not significant (within one standard deviation). This could imply that the physical mechanism responsible by this abnormal occurrence is not continuous or persistent, but is one of a sporadic nature. Large solar activities seem to often occur in July and November. As examples, we could mention the Bastille event (July 2000, ($Dst = -301$)) and the Halloween events (October–November 2003, (Dst ~ −400)); also, *Willis et al.* [1997] used the *aa* index to investigate the largest geomagnetic storms per solar cycle within the period 1844–1993, solar cycles (SCs) 9–22. Among 14 SCs the first maximum in *aa* index was found to occur in July or November four times: 20 November 1882 ($aa = 304.6$, SC12), 20 July 1894 ($aa = 220.6$, SC13), 8 July 1928 ($aa = 278.3$, SC16), and 13 November 1960 ($aa = 352.1$, SC19). We could also mention other large events: 12 July 1982 ($Dst = -325$), 16 November 1989 ($Dst = -266$), and 4 November 2001 ($Dst = -292$).

3.2. Annual Dependence of Solar Wind Parameters

[13] Figure 3 shows the monthly averages of magnetic field strength (B), T_p, V_{sw}, and N_p calculated from the OMNIweb data during 1973–2000. Error bars are also shown. One standard deviation, calculated from the monthly averages of all years, is around 1.1 nT for B, 33×10^3 K for T_p, 1.8 cm^{-3} for N_p, and 52 km s^{-1} for V_{sw}. The dotted lines on Figure 3 indicate the parameter averages for the period between 1973 and 2000: $N_p = 9.3$ cm^{-3}, $B = 6.7$ nT, $V_{sw} = 445$ km s^{-1}, and $T_p = 86 \times 10^3$ K. These values are shown in Table 1, conjoint with range variations, for the whole and solar minimum and maximum periods. The observed variations in standard deviation can be accounted for by the solar cycle variations (11- and 22-year) and by the long-term variability, reflecting different solar wind environments [*Gazis*, 1996; *Zieger and Mursula*, 1998].

[14] Results presented in Figure 3 indicate a slight asymmetry in solar wind parameters, regarding the first and the second half year. The peak to peak variations (range from the maximum to minimum values) for the parameters are $\Delta N_p \approx 1.7$ cm^{-3} (≈18%), $\Delta B \approx 0.8$ nT (≈12%), $\Delta V_{sw} \approx 37$ km s^{-1} (≈8%), and $\Delta T_p \approx 16 \times 10^3$ K (≈18%). V_{sw} and T_p present higher values during the first half year, decreasing along the remaining months. The opposite happens with

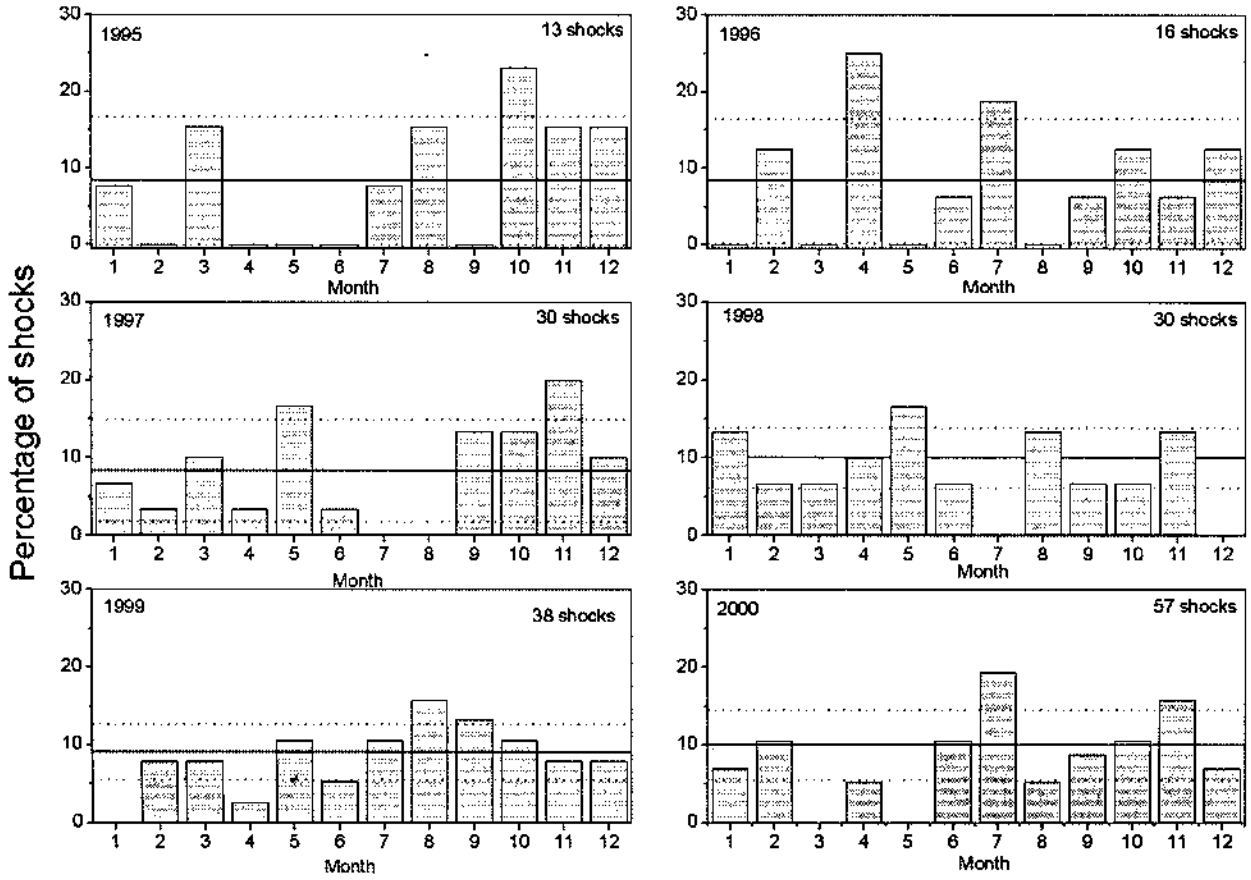

Figure 2. Monthly occurrence of interplanetary shocks near 1 AU for 6 sequential years in a half of a solar cycle. Percentage of shocks per months is plotted for 1995, 1996, 1997, 1998, 1999, and 2000. Average and one standard deviation of shock occurrence are indicated by the solid and dotted lines, respectively.

N_p, which presents lower values during the first half year. While plasma parameters show an annual variation as the predominant behavior for the whole data period, B shows a different variation: a semiannual variation with two maxima (in February and in November) and a deep minimum in July. The qualitative behavior of V_{sw} is similar to the one found by *Zieger and Mursula* [1998] during solar minima 1975–1976 and 1994–1995, probably because solar wind observations are sparser during the alternate solar cycle minima in the 1960s and in the 1980s.

[15] Figure 4 shows an idealized representation of the geometry of the Sun in relation to the Earth according to the epoch of the year. Because of the 7.2° inclination of the Sun's axis of rotation relative to the ecliptic plane, during the course of 1 year the rotational Sun's axis is differently seen by the Earth. The Earth's heliolatitude is maximum in early September, minimum in early March, and zero at the beginning of June and December. This causes an observer on the Earth to be located above or below the Sun's equator depending on the time of year. Consequently, Earth is exposed each half year to different solar hemispheres, which are known to have opposite magnetic polarities that reverse each ~11-year solar cycle. It is known that V_{sw} increases by 2–10 km s^{-1} per degree of latitude away from the solar equatorial plane [*Newkirk and Fisk*, 1985; *Bolton*, 1990], and a symmetrical semiannual variation should be expected. From Figure 3 a minimum in V_{sw} is observed around July, but the "second peak" (September) of the expected semiannual variation in V_{sw} is absent.

[16] The difference in plasma parameters observed during the two half years are indicative of difference in solar magnetic hemispheres. Furthermore, as the annual variation is present mainly in alternate solar minima, when a given solar hemisphere has the same magnetic polarity, the observed asymmetry is between the positive and negative solar magnetic poles. It is well known that the global magnetic field changes its polarity around solar maximum (the 22-year Hale solar magnetic cycle). In order to have data related to the same polarity of solar magnetic field, or the same Hale 22-year solar cycle phase, we obtained the annual distribution of solar wind parameters for intervals from a solar maximum to another. The obtained distributions can be seen in Figure 5. A semiannual variation is clearly seen for V_{sw} for the period 1980–1989, while for the other two studied periods an annual variation should better

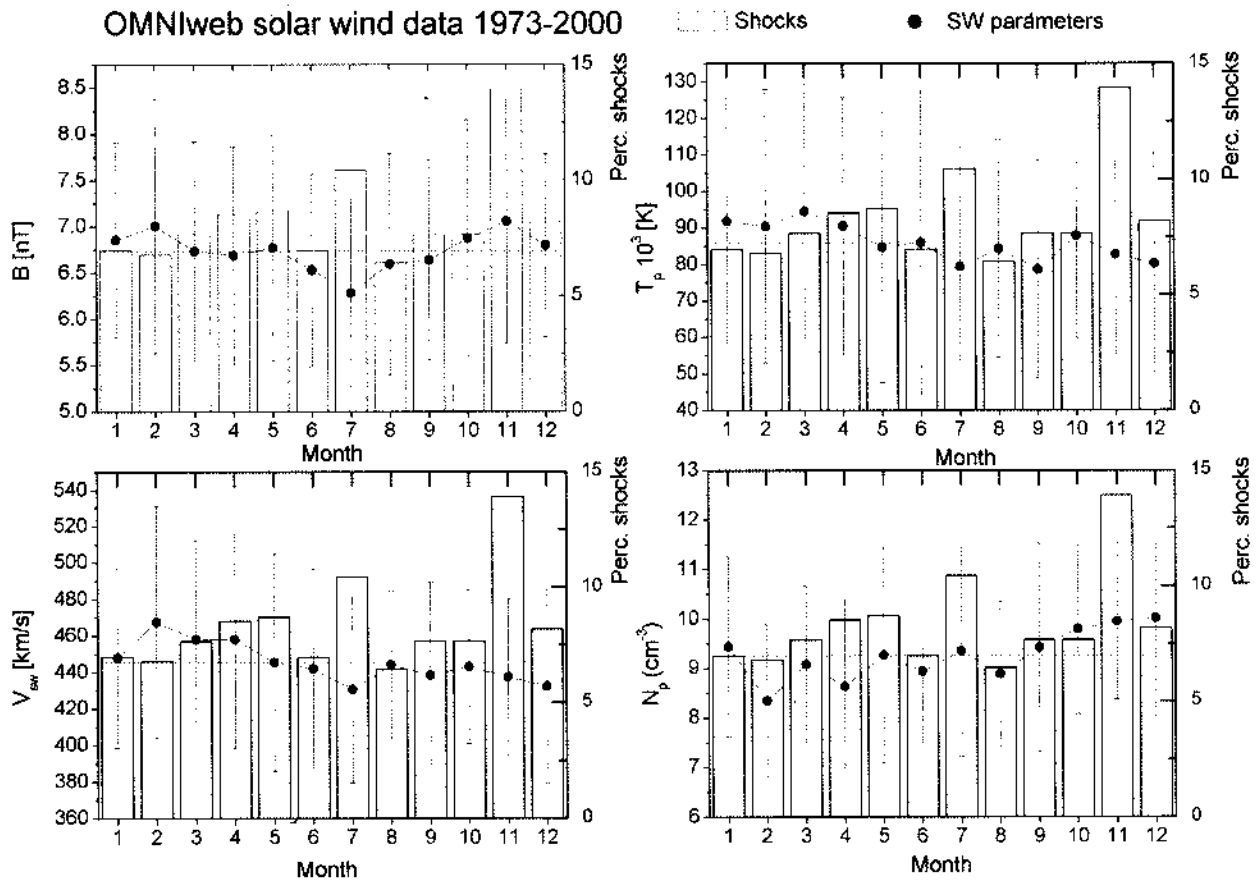

Figure 3. Monthly averages of solar wind parameters during 1973–2000 period. Dotted lines are the averages for the whole period. Shock distribution is also plotted, as column bars.

describe the behavior. The annual variation shape in solar wind speed was shown by *Zieger and Mursula* [1998] to be different from one phase to another in the Hale 22-year solar cycle.

[17] Figure 6 shows the solar wind parameter variations for the different solar cycle minimum and maximum epochs mentioned above. Differences can be seen between solar maximum and minimum, both in the absolute values of parameters (reflecting different phases and different 11- and 22-year solar cycles) and in the profiles. During solar maximum the profiles are more irregular for all parameters. These findings confirm the ones reported by *Zieger and Mursula* [1998] regarding the annual variations of solar wind speed. It can be seen that around solar minimum, solar wind parameters show a very clear annual variation, while around solar maximum they have a highly irregular behavior. A semiannual variation is observed for B profiles, with minimum around July and peaks in February and November, for both epochs.

[18] Results presented in Figures 3 and 6 are summarized in Table 1. Average values and peak to peak variation (between parentheses) are shown for the whole period and also for solar minimum and maximum periods. From Table 1 it can be seen that solar wind plasma parameters, on average, are higher during solar minimum, except for B, which is higher during solar maximum. Ranges of variation are as follows for solar maximum (minimum): in B, 12.3% (11.3%); in T_p, 37% (33%); in N_p, 26% (16%), and in V_{sw} 8.6% (12%).

[19] Linear correlation coefficients between shock rate and solar wind parameters for the whole period are low: −0.42 (V_{sw}), −0.38 (T_p), +0.49 (N_p), and +0.16 (B). These low correlation coefficients indicate that the solar wind parameter variations are not the whole explanation of shock distribution. Linear correlation coefficients between solar wind parameters and shock rate are usually higher in solar minimum than in solar maximum.

[20] During solar maximum (minimum), correlation coefficients with shock rate are as follows: for B, +0.28 (+0.51); for T_p, +0.26 (−0.42); for N_p, +0.13 (+0.53), and for V_{sw}, +0.14 (−0.34). A direct physical significance can be attributed to the anticorrelation observed between shock rate and

Table 1. Averages and Ranges for Solar Wind Parameters

Parameters	Averages (Ranges)		
	1973–2000	Solar Minimum	Solar Maximum
V_{sw}	445 (37) km s^{-1}	450 (55) km s^{-1}	420 (36) km s^{-1}
T_p	86 (16) × 10^4 K	90 (30) × 10^3 K	76 (28) × 10^3 K
N_p	9.3 (1.7) cm^{-3}	9.2 (1.5) cm^{-3}	8.7 (2.3) cm^{-3}
B	6.7 (0.8) nT	6.1 (0.7) nT	7.0 (0.9) nT

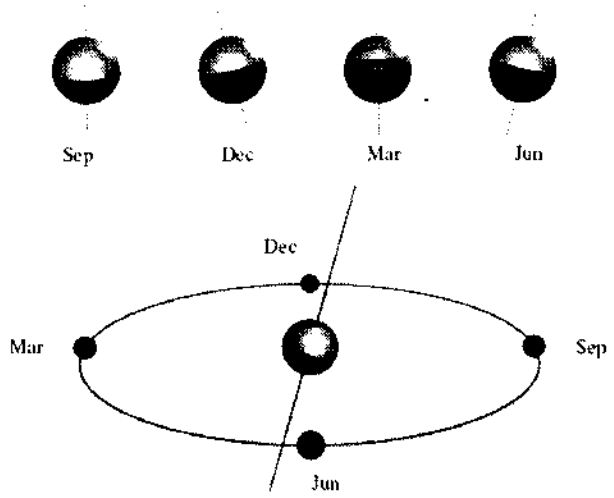

Figure 4. Illustrative sketch of the Sun-Earth geometry during 1 year. (top) A "view" of the Sun by Earth in different epochs of year is shown. Around the beginning of March the solar southern hemisphere is more visible, while around the beginning of September the solar northern hemisphere is more visible. (bottom) Around the beginnings of June and December, Earth is crossing the solar equator. Solar rotation axis is represented in figures. Inclined and shaded plane is the heliographic equator (approximately the heliomagnetic), while the ecliptic plane is delimitated by the Earth's orbit.

V_{sw} in the entire period and during solar minimum (despite a very low positive correlation in solar maximum), because it is expected that when the solar wind speed is lower, there is a higher probability of shock formation. The other plasma parameters are not directly connected to shock formation. However, they are relevant when defining the characteristic speeds.

[21] Linear correlation coefficients between different pairs of monthly average of solar wind parameters are shown in Table 2, for the whole period and for the solar maximum and minimum epochs (data from Figures 3 and 5). The highest correlations are obtained between V_{sw} and N_p and V_{sw} and T_p. Except for the correlations including B, they are higher during solar minimum than solar maximum. This can be explained by the irregular variations seen during solar maximum period contrasted with the smooth variations during solar minimum. Correlations between B and solar wind plasma parameters are less significant, lower than 0.5.

[22] The T_p and V_{sw} correlated and the N_p and V_{sw} anticorrelated variations were expected. It has been observed that along a solar cycle, N_p is more or less constant, while T_p variations are correlated with V_{sw} [*Gazis*, 1996]. The origin of this behavior is not fully understood, although it has been suggested that the T_p-V_{sw} correlation should be accounted for by the distance from the heliospheric current sheet, HCS [*Gazis*, 1996; *Smith*, 2001]. The HCS separates regions of the solar wind where the magnetic field points toward or away from the Sun. The heliospheric current sheet persists into the outer heliosphere and is responsible for both local and global phenomena in the solar wind. Moreover, for a uniform plasma density at the base of the corona, easier escape of the plasma particles will cause the plasma density on open field lines to be smaller (and the outflow speed larger) than on closed field lines at the same distance from the Sun. Close to the heliospheric plasma sheet of the HCS, N_p values are higher and V_{sw} are lower [*Winterhalter et al.*, 1994]. Thus if the distance to the HCS really influences the average solar wind plasma parameters, it is expected for V_{sw} and N_p to be anticorrelated.

[23] Differences in the behavior of solar wind parameters during solar maximum and minimum can be easily seen in Figure 6. It is observed that magnetic field strength is higher during solar maximum than during solar minimum, but plasma parameters are higher during solar minimum. It might be expected from the anticorrelation between N_p and V_{sw} that their solar cycle behavior should be different, with higher V_{sw} coincident with lower N_p, but this is not observed in Figure 6. However, it is well known that this anticorrelation over short timescales does not seem to be maintained along a solar cycle period [*Gazis*, 1996].

[24] These results and the ones seen in Figure 3 show that the annual variation found by *Zieger and Mursula* [1998], although stronger and visible in alternate solar cycle minima, is visible even by taking averages along solar minimum or in the whole solar wind observational periods. This implies that the amplitude of the annual variation is stronger than the irregular variation amplitudes seen in other periods.

[25] Variations in plasma and magnetic field parameters could have implications in the solar wind propagation conditions and consequently in shock formation. The lower V_{sw} found in second half year can be particularly favorable to shock formation. The necessary condition of shock formation is that the velocity difference between the wave (shock) driver and the background medium should be higher than the characteristic medium speed. Also, B and N_p variations can have important influence on shock formation since they define the characteristic speeds of the medium. Alfvenic and magnetosonic speeds of the solar wind have been then calculated from the monthly average parameters. The Alfvén speed is calculated from [*Kennel et al.*, 1985]

$$V_A = \frac{B_1}{\sqrt{\mu_0 \rho_1}}. \tag{1}$$

[26] In equation (1), B_1 is the total magnetic field, and ρ_1 is the plasma density in the upstream side. The magnetosonic wave speed is given by

$$V_{MS} = \left\{(1/2)\left(V_A^2 + C_S^2\right) \pm \left[\left(V_A^2 + C_S^2\right)^2 - 4C_S^2 V_A^2 \cos^2(\alpha)\right]^{1/2}\right\}^{1/2}, \tag{2}$$

where C_s is the sound speed and α is the angle between the propagation direction of the wave and the environmental upstream magnetic field. Only the positive solution (signal plus sign) is used in order to obtain the fast-mode magnetosonic speed. In the case of the magnetosonic wave steepening in shock wave, α would be the angle between the shock normal and $\mathbf{B}_1$. Three angles were taken to

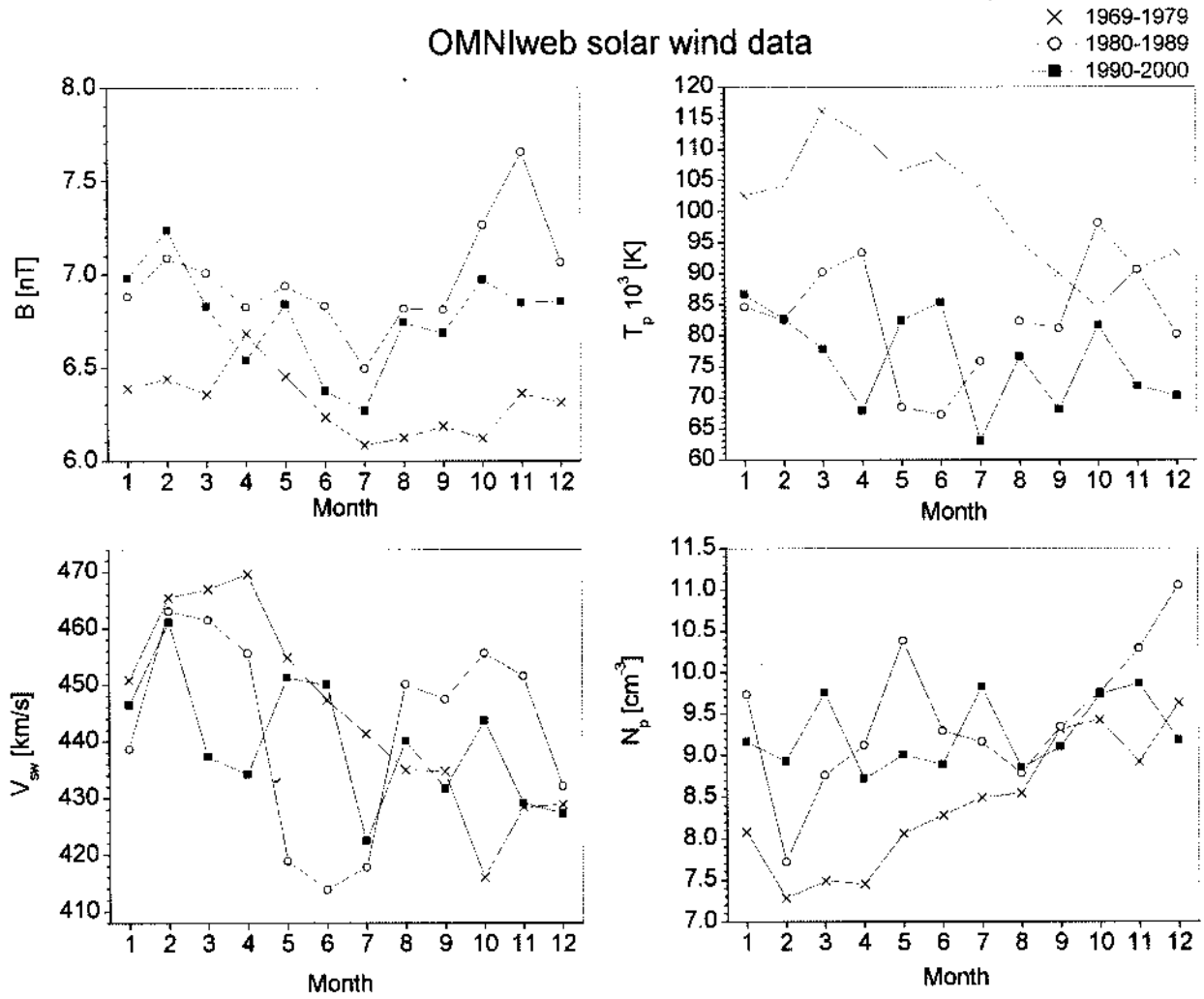

Figure 5. Monthly averages of solar wind parameter for solar cycles defined from one maximum to another: 1969–1979, 1980–1989, and 1990–2000.

calculate V_{MS}: $\alpha = 0°$, $\alpha = 45°$, and $\alpha = 90°$, encompassing parallel, oblique, and perpendicular shocks, respectively.

[27] Figure 7 shows the 1973–2000 average profiles for solar wind characteristic speeds. Notice that every characteristic speed shows a trend to be lower during the second half year. A maximum is observed around February and a deep minimum around July. Although for November the values are not very different from the average, there is a minimum in December. The relative annual variation for V_A and V_{MS} is around 10–15%. These lower values in July could be used to explain the shock rate peak. In general, the second half year shows lower characteristic speeds than the first half, which can be indicative of more favorable shock formation conditions.

[28] Distributions of solar wind characteristic speeds were also determined for solar minimum and maximum periods and are shown in Figure 8. The profiles are observed to be more irregular around solar maximum years because of the irregularities in solar wind parameter distributions. Nevertheless, low values are seen around July for every characteristic speed, while for November the values are not so low. Solar maximum characteristic speeds were observed to be slightly higher than during solar minimum. This could imply easier shock formation conditions during solar minimum, if shocks were expected to occur with the same frequency and strength as during solar maximum; actually, however, the number of shocks is known to vary in phase with the solar cycle [*Webb and Howard*, 1994]. For solar minimum period, variations were observed to be smoother than for solar maximum, as expected from the observed solar wind variation, with a minimum in July for V_A and V_{MS}. While solar maximum parameters had a variation with a minimum in July, for solar minimum, second half year values are lower than first half year, similar to the whole period (Figure 8). Characteristic speeds are higher during solar maximum than in solar minimum. Average values for solar maximum (solar minimum) are V_A = 52 (44) km s^{-1}, V_{MS} (0°) = 60 (48) km s^{-1}, V_{MS} (45°) = 69 (63) km s^{-1}, and V_{MS} (90°) = 75 (69) km s^{-1}. This implies easier shock formation conditions during solar minimum. A similar result was found in a previous work [*Echer et al.*, 2003] when a comparison between shock parameters during solar

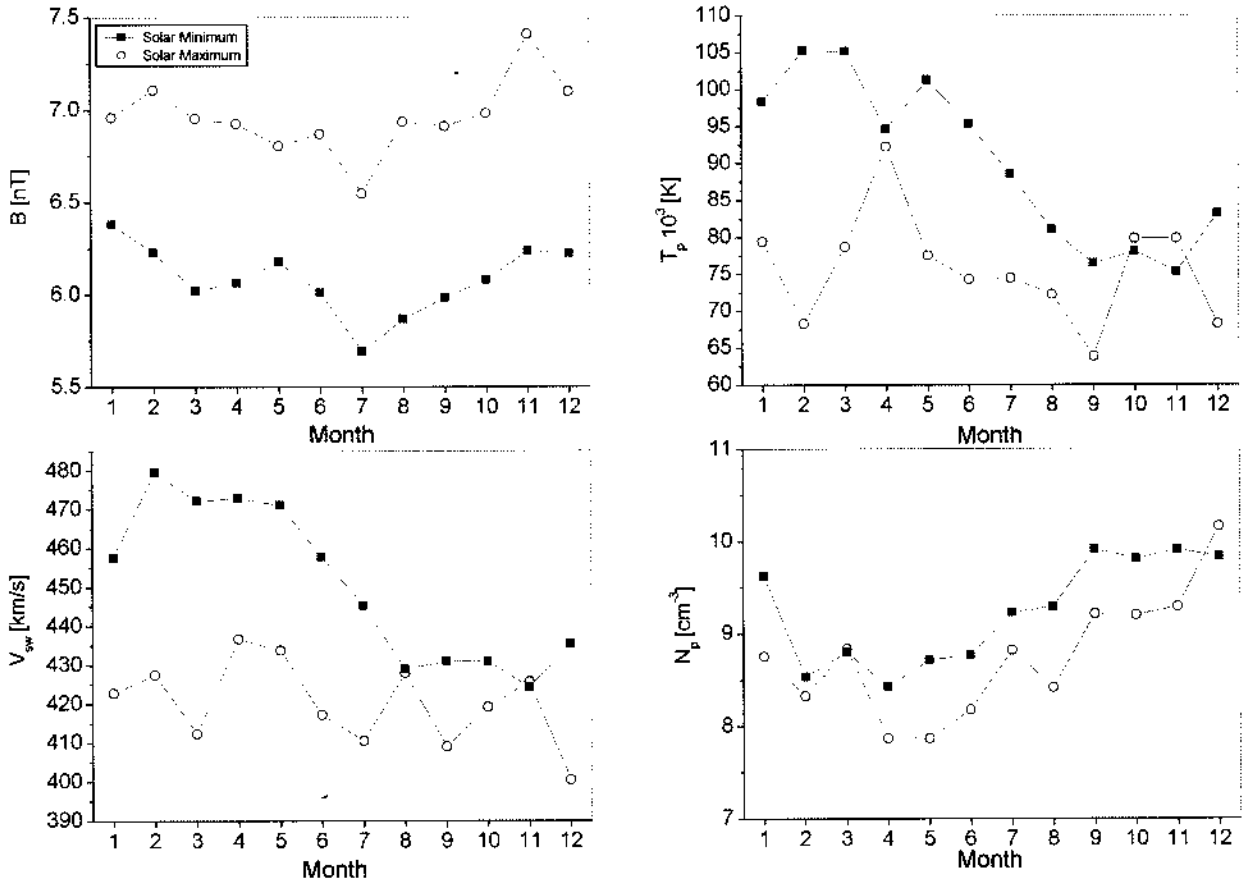

Figure 6. Monthly averages of solar wind parameters around solar minimum (1973–1978, 1993–1998, line with solid squares) and solar maximum (1977–1982 and 1998–2000, line with open circles) periods.

minimum 1995–1996 years and maximum 2000 year was done. In that work it was observed that the Alfvenic Mach number of shocks was, on average, similar during solar maximum and minimum years. This occurs because, despite the higher shock speeds during solar maximum, the higher N_p values during minimum makes V_A lower during solar minimum and the formation of shocks easier.

3.3. Annual Variation in Very Intense Geomagnetic Activity

[29] The geomagnetic activity has a very well known semiannual variation, with peaks around equinoxes [*Russell and McPherron*, 1973]. Three mechanisms are taken into account to explain the variations: the axial, the equinoctial, and the Russell-McPherron hypothesis. Nevertheless, *Clúa de Gonzalez et al.* [2001, 2002] have shown that the distribution of occurrence of intense storms shows deviations from this behavior, with additional peaks in July and in November. Figure 9 shows a comparison of the seasonal variation of interplanetary shocks occurrence and intense geomagnetic activity during 1973–2000: Figure 9 (top), number of days per month for $aa \geq 90$ to $aa \geq 150$ levels; Figure 9 (middle), number of geomagnetic storms considering Dst peak ≤ -150 to $Dst \leq -190$ nT levels; and Figure 9 (bottom), number of events with $AE \geq 1700$ nT during 1973–1994. Geomagnetic indices are represented by the line with different symbols related to the levels of activity while the shock occurrence is the bar diagram graph. Notice that for this interval, shorter than the whole period calculated by *Clúa de Gonzalez et al.* [2001, 2002], the number of points is reduced and the correlations are then less significant. Particularly, the levels of $aa > 180$ and $aa > 210$, considered by *Clúa de Gonzalez et al.* [2001, 2002], had such a small number of points (nine and three, respectively) that they are not shown here.

[30] For the period analyzed in this paper, the July peak is clearly visible for all indices, being more pronounced for the AE index. For the aa and Dst indices the semiannual variation is predominant, although an increase in the number of events that occurred in July can be observed when the index threshold is increasing. The November peak is also

Table 2. Linear Correlation Coefficients Between Solar Wind Parameters

Parameters	1973–2000	Solar Minimum	Solar Maximum
$V_{sw}XN_p$	−0.76	−0.89	−0.78
$V_{sw}XT_p$	+0.83	+0.96	+0.59
$V_{sw}XB$	+0.40	+0.21	+0.11
N_pXT_p	−0.48	−0.81	−0.42
N_pXB	+0.16	+0.12	+0.38
T_pXB	−0.38	+0.22	+0.01

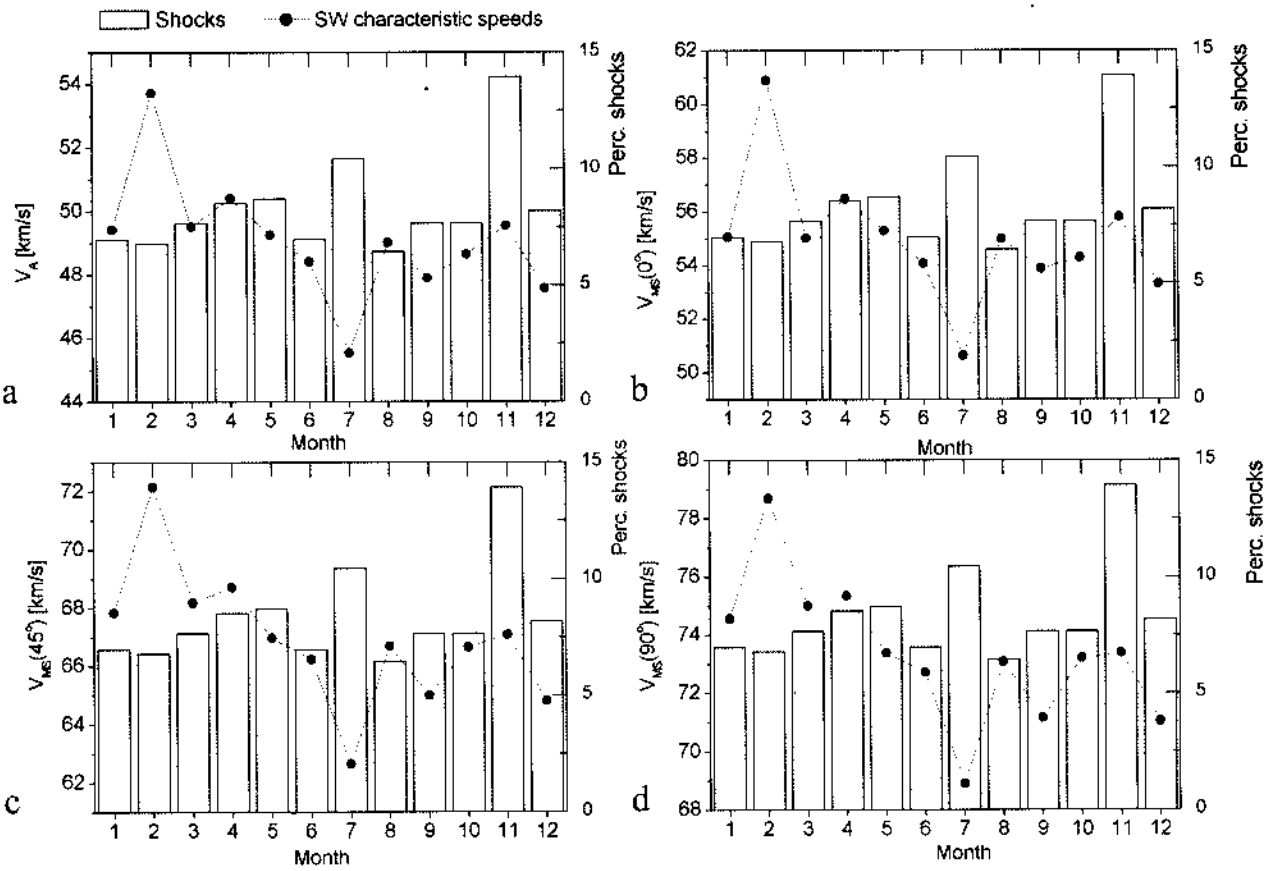

Figure 7. Monthly averages of solar wind characteristic speeds during the 1973–2000 period. (a) Alfvén speed, magnetosonic speed for assumed three different angles between the wave front and the background magnetic field: (b) 0°, (c) 45°, and (d) 90°. Shock distribution is also plotted, as column bars.

observed for the *AE* index; when increasing the *aa* threshold, it starts to be comparable to the September and March equinoctial peaks (*aa* > 150). The November peak is not present for the *Dst* index. The mechanism responsible for this anomalous distribution is not known, but a possible explanation was considered to be a hemispheric/seasonal asymmetry in ionospheric conductivity [*Clúa de Gonzalez et al.*, 2001]. *Sonnemann* [2002] refers to these irregularities as geomagnetic singularities and attributes its origin to atmospheric asymmetries.

[31] Nevertheless, the peaks in the shock annual distribution in July and November are coincident with the peaks in the very intense geomagnetic activity (as shown for *aa* > 150 and *AE* > 1700), which could indicate a causal mechanism. Shocks are a proxy of geoeffective interplanetary structures, fast interplanetary coronal mass ejections and/or magnetic clouds [*Gonzalez et al.*, 1999]. Further, intense fields can occur in the sheath region, behind the shock, and be responsible for intense magnetic storms. Particularly, it has been shown that most of the very intense geomagnetic storms (*Dst* < −200 nT) are associated with or caused by fields in the sheath region, originated from compression mechanisms [*Tsurutani et al.*, 1992]. As a consequence, since after a shock the solar wind plasma is compressed and the magnetic field is intensified, the energy transfer between solar wind and magnetosphere is modified, causing a larger number of intense magnetic activity events as indicated by geomagnetic indices. Since the irregular peaks in geomagnetic activity are also a statistical effect, not occurring every year, the sporadic higher rate of interplanetary shocks in July and November during some years could account for a higher number of intense geomagnetic storms during the same years in July and November.

[32] The peaks in the very intense geomagnetic activity recorded by *aa* and *AE* could be explained not only by intense and long duration southward magnetic fields, but also by effects of the strong compression of magnetosphere by shocks. The intensification of magnetospheric currents (magnetopause, field-aligned, cross tail) can occur due to a jump in the solar wind dynamic pressure. There are also recent evidences that substorms are triggered by shocks [*Tsurutani and Zhou*, 2003; *Zhou and Tsurutani*, 2001, 2002].

[33] Geomagnetic indices variation does not follow quite well the interplanetary shock occurrence variation (Figure 9), but the peaks in July and also in November (less clear for *Dst*) in geomagnetic activity have a correspondent peak in shock occurrence. It can not be expected that the shock annual distribution explains the whole yearly variation in geomagnetic activity, since the semiannual signal is still the main characteristic. Correlation coefficients are very low for most of the levels, being higher only for more intense

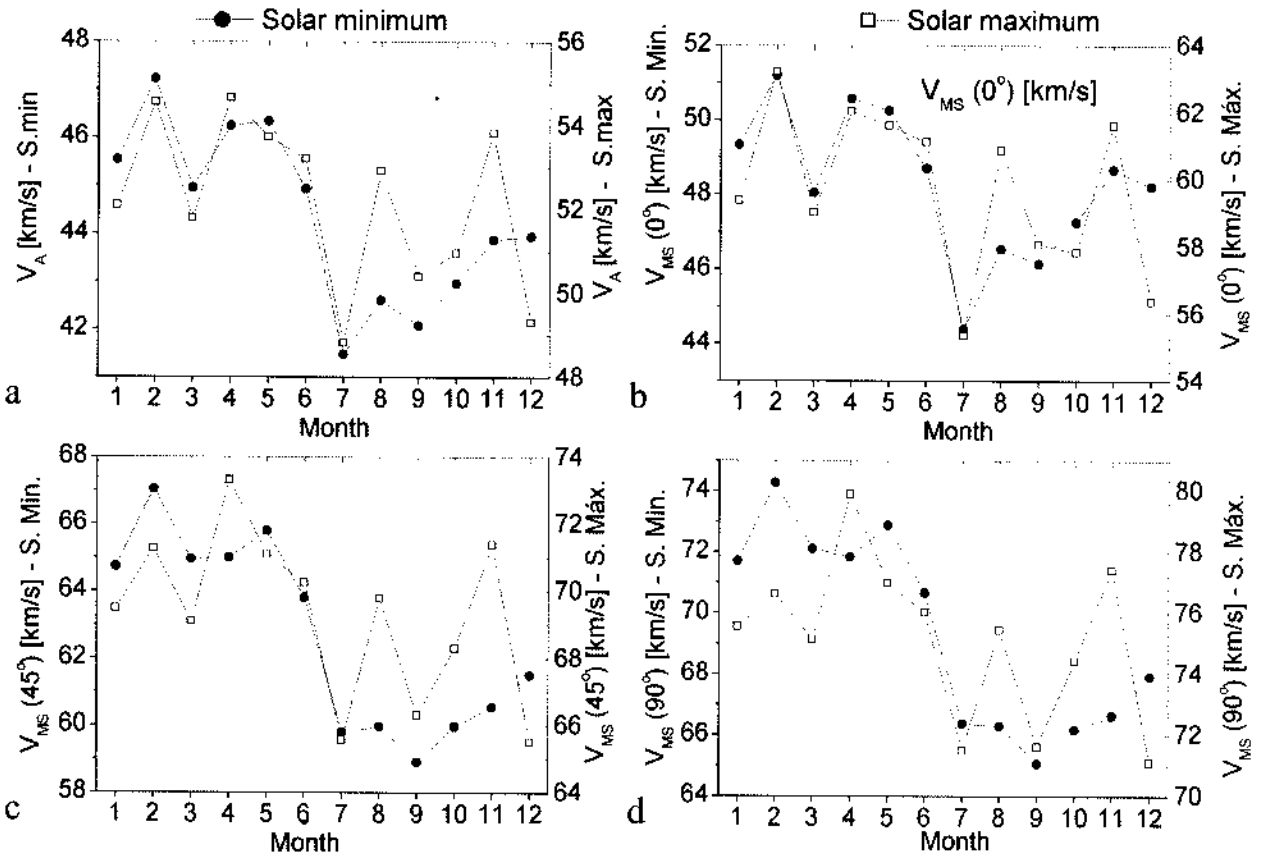

Figure 8. Monthly averages of solar wind characteristic speeds for solar minimum and maximum periods. Panels are: (a) Alfvén speed, magnetosonic speed for assumed three different angles between the wave front and the background magnetic field: (b) 0°, (c) 45°, and (d) 90°.

magnetic activity. Linear correlation coefficients more significant are 0.48 and 0.39 for $aa > 120$ and $aa > 150$ levels, 0.42 for $AE > 1700$, and 0.22 for $Dst \leq -190$ nT level. For the other levels, coefficients were lower than 0.1. This result implies that the shock rate distribution can at most explain a small part of the geomagnetic activity variation: <20% (highest $r = 0.48$) along the entire year.

3.4. Possible Solar Contribution

[34] Solar activity variations exhibit themselves in electromagnetic radiation from radio frequencies of a few kilohertz to powerful gamma rays and also in particle flux. In particular, these variations can be quantified by the H_α flare index, which can be represented by $Q = it$, where i represents the intensity scale of importance of a flare in H_α, and t represents the duration in H_α (in minutes) of the flare [*Özgüç et al.*, 2002]. This quantitative index may be roughly proportional to the total energy emitted by the flare. Using data available from National Oceanic and Atmospheric Administration/National Geophysical Data Center, we constructed the annual variation for the H_α flare index for the same periods we have obtained the shock rate. Results are shown in Figure 10. It is interesting to observe the presence of peaks in July and November for the whole period and also for the solar maximum period. For solar minimum period, only the November peak is present. The annual behavior of the H_α flare index is very similar to the annual shock rate. Since the H_α flare index is a measure of the total energy emitted by the flare, maybe the November peak is more related to the Sun activity. This result might imply a solar activity contribution to the shock formation. However, CMEs and not flares are known to be the shock drivers, and, since flares and coronal mass ejections are not always related [*Gosling*, 1993], it would be necessary to assess the CMEs' rate annual variation to test if this distribution is also observed.

4. Discussion and Conclusions

[35] In this section, the possible causes for the observed asymmetry in shock rate near 1 AU are discussed. It is suggested that this asymmetry may have different sources of explanation. Our results show that one of the reasons is linked to the solar wind parameter annual dependence. Solar wind plasma parameters, V_{sw}, T_p, and N_p, show clearly an annual variation for the whole analyzed period and for the solar minimum periods (Figures 3 and 6). Solar wind speed tends to be higher around March equinox than around September equinox, especially during alternate solar minimum periods [*Zieger and Mursula*, 1998]. As a consequence the solar wind emitted from north and south solar hemispheres will present different properties, reflected

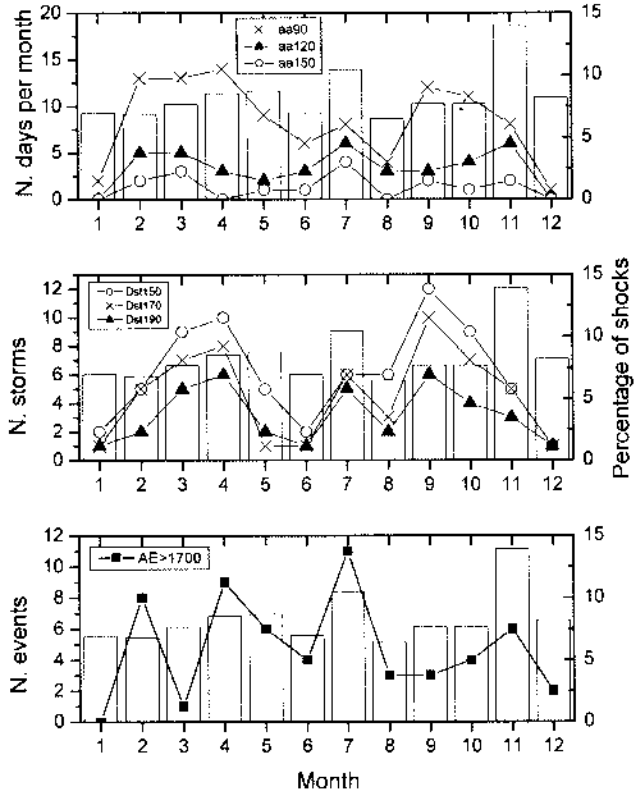

Figure 9. Comparison of the seasonal variation of interplanetary shocks occurrence and intense geomagnetic activity during 1973–2000: (top) *aa* levels ($aa \geq 90$ to $aa \geq 150$); (middle) *Dst* peak ≤ -150, -170, and -190 nT; and (bottom) $AE > 1700$ nT (1973–1994). Geomagnetic indices are represented by the line with different symbols for different levels of activity, while the shock occurrence is column bars.

on solar wind parameters, as can be seen in Figures 3, 5, and 6.

[36] Earth's orbit has its aphelion during July (1.017 AU = 152.1×10^6 km) and its perihelion during January (0.98 AU = 147.1×10^6 km). The average distance or 1 AU is 149.6×10^6 km. Using the model of Parker for the steady solar wind expansion [*Parks*, 1991], magnetic field varies as $B \sim 1/r^2$, and we obtain $B_{aph}/B_{1AU} = 1.034$ and $B_{per}/B_{1AU} = 0.967$, the total difference being of order of 7%. This first approximation gives then a variation in B near Earth's orbit due only to the varying radial Sun-Earth distance. Comparing these calculated results with the observed variations, it can be noticed that the radial dependence is able to explain part of B variations. The observed enhanced variation from aphelion to perihelion is $\Delta B \approx 5\%$. Other factors should be operating, such as the heliographic dependence of Earth's orbit.

[37] Considering the above discussion, it is possible to say that the solar wind parameter annual dependence have the following as possible causes: the radial dependence because of the varying Sun-Earth distance (for B) and the heliographic latitude (Earth is at its maximum angular distance (~7°) from solar equatorial plane and thus more closely aligned with both the sunspot zone and coronal holes that extended down from the solar poles, around equinox).

[38] The lower solar wind and characteristic speeds observed in the second half year, for the whole period analyzed in this paper and for the solar minimum periods (Figures 3 and 6), suggest an asymmetric propagation condition in heliosphere, close to Earth's orbit. This could determine more favorable conditions for shock formation during the second half year. Interplanetary ejecta can drive a shock if its relative speed to the solar wind is larger than the characteristic speed of the medium (V_A and V_{MS}). If ejecta are emitted by the Sun at the same rate every month of the year, with the same intensity and velocity, then the relative speed of interplanetary ejecta will depend only on solar wind speed. Thus one can expect that in the second half year the relative speed between ejecta and solar wind will be larger, because of the lower solar wind speed. The other plasma parameters also vary in a way of causing lower V_A and V_{MS} in the second half year. All this implies that shock formation should be easier in the second half year. Particularly, in July, the characteristic speeds of the medium are much lower when compared to the other months, for the whole period analyzed in this paper (Figure 7) and for the solar maximum periods (Figure 8). However, this particular is not observed for the minimum periods (Figure 8), which

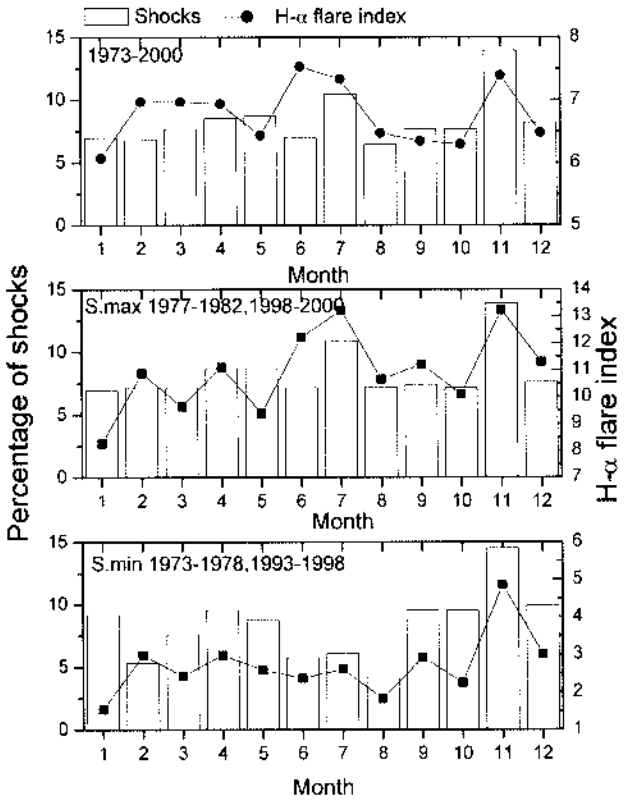

Figure 10. Comparison of the seasonal variation of interplanetary shocks occurrence and the H_α flare index during 1973–2000: (top) 1973–2000; (middle) solar maximum, 1977–1982, 1998–2000; and (bottom) solar minimum, 1973–1978, 1993–1998. H_α flare index is represented by the line with solid circle points, while the shock occurrence is column bars.

shows a lower solar wind speed during the entire second half-year period. All these arguments of more favorable conditions for driving a shock could explain the shock rate peak observed in July, but not the November peak, which has as a possible factor for easier shock formation only lower than average solar wind speeds. However, the annual variation of H_α flare index clearly presents a peak in November, reflecting a larger amount of energy been emitted from the Sun. This might imply a higher fast CME rate driving interplanetary shocks, but a future investigation is necessary to assess this point.

[39] Linear correlation coefficients between shock rate (SR) and characteristic speeds were obtained, and the results indicate negative and low correlations: SR × V_A, $r = -0.23$; SR × V_{MS} (0°), $r = -0.20$; SR × V_{MS} (45°), $r = -0.28$; SR × V_{MS} (90°), $r = -0.29$. The negative correlation is expected, because the SR will be higher when the characteristic speed is lower. However, the coefficients are very low, indicating that <10% of SR distribution could be explained by a linear dependence on characteristic speeds only. The correlation between SR and V_{sw} is slightly higher, $r = -0.42$ (lower solar wind speeds, more favorable shock formation conditions). By taking a multiple linear correlation of SR with V_{MS} (45°) and V_{sw}, one has $r^2 = 0.26$ ($r = -0.51$), implying that 26% of the SR annual distribution can now be explained by a linear dependence of both the solar wind speed and the magnetosonic speed. This indicates that 75% of SR variance is yet not explained, which just shows how complex the problem is. At the same time it is remarkable that when one takes long-term averages it is possible to have an explanation of 25% of variance by these simple considerations. Irregularities in the solar wind and the coronal mass ejection rate from the Sun (as well as other possible solar sources of shocks: blast waves, interaction regions) are processes not being taken into account in these analyses.

[40] The annual variation in the heliospheric current sheet close to the Earth can be observed by the variation in the polarity structure of the sectors as reported by *Wilcox and Scherrer* [1972] and *Rosenberg and Coleman* [1969]. The predominant *B* polarity should be the same as the solar polar region pointed to the Earth and should be reverted around 7 June and 7 December. The occurrence of sector boundary crossings (SBC) also shows a semiannual variation [*Sawyer*, 1974], with more sectors per rotation in May–June and in November–December, which are periods when Earth is crossing the heliospheric equator and which are approximately the periods with more shocks. Nevertheless, it is important to consider that the model of a flat, well behaved HCS is valid only during solar minimum, because during solar maximum the heliosphere is highly disturbed, and the HCS is known to have an irregular pattern, with large amplitude warps/waves. Furthermore, it was recently shown that the annual variation in the *B* polarity is present only during the rising solar cycle phase, being absent in the descending phase [*Echer and Svalgaard*, 2004].

[41] *Mendoza and Pérez-Enríquez* [1995] have studied the storm sudden commencements (SSC) variations and they have determined that SSC events tend to accumulate around the day of the Earth's crossing of the HCS (sector boundary crossing). They also observed that around 40–50% of SSC events and sudden impulses (SI) occur within the first day from SBC. As SSC and SI are mainly caused by interplanetary shocks, these results indicate that many shocks occur when Earth is close to the HCS. Also, the HCS is the preferential region where ICMEs occur. *Fengui and Dryer* [1991] analyzed 149 shocks associated to flares and also observed that these shocks tend to propagate to the low heliolatitude/solar equator; they have also noticed that the faster propagation direction tends to be close to HCS around 1 AU. *Eselevich and Filippov* [1988] suggested that the Alfvenic velocity is low close to and inside the HCS around 3 solar radiuses. Thus the supermagnetosonic shock speed would be more probable to be reached in this region than in other heliolatitudes. These results suggest that an easier shock formation might occur in the proximity of the HCS, and this process could result in lower solar wind speeds and higher proton density observed in the heliospheric plasma sheet of the HCS [*Winterhalter et al.*, 1994].

[42] Another possibility to be taken into account to explain the observed annual variation of SR could be some internal process in the Sun. For instance, there are suggestions that major solar flares are not random on the solar surface but are concentrated in active zones or hot spots [*Bai*, 1990]. The small changes in Alfvenic/magnetosonic parameters may be not enough to account for SR variation, and this variation may be associated with changes at or near the solar wind source region. Perhaps CMEs associated with shocks were simply more common at low southern heliographic latitudes around July in solar maximum periods, either because CMEs themselves were more common or CMEs were more likely to produce significant shocks that were observable at 1 AU. The H_α flare index annual distribution presents a good agreement with shock distribution, providing a hint of a solar contribution. An analysis of the CMEs and other solar sources generating shocks in the last decade would be necessary to test the case of a solar source variation. Nevertheless, if a solar annual variation is also confirmed, it opens another question, namely which is the cause of solar flares (and maybe CMEs) to have an annual dependence.

[43] In summary, an unexpected annual variation in interplanetary shock rate near Earth's orbit was found in this study, with preference occurrence (statistically) in July and November, when Earth was at heliographic latitude of ~3°N, and it was more pronounced in November than in July. This variation was more noticeable in the vicinity of the 1979 and 2000 solar maxima. A detailed analysis of solar wind and IMF parameters was performed. The annual variation was found to be comparable with the shock rate in a wide range of solar wind and IMF parameters. Results show that the second half year presents more favorable propagation conditions for shocks, which could partially explain the observed asymmetry in shock rate. These conditions are lower solar wind bulk speeds and also lower characteristic speeds, both Alfvenic and magnetosonic, when compared to average values. Besides solar wind variation the similar variation in shock rate and H_α flare index might imply a solar origin contribution to shock variation. Furthermore, the peak in very intense geomagnetic storms found by *Clúa de Gonzalez et al.* [2001, 2002] in July and November could be accounted for by this shock rate distribution. It is suggested that further studies should be conducted, both observational and theoretical/modeling,

in order to assess this solar wind asymmetry, which seems to have origin in slight differences in opposite solar magnetic hemispheres.

[44] **Acknowledgments.** Thanks to the National Space Science Data Center (NASA/Goddard) for the OMNIweb data set. Thanks to National Geophysical Data Center and to the World Data Center-Geomagnetism for the *aa*, *AE*, and *Dst* geomagnetic indices, and the H_α flare index. Thanks to FAPESP for postdoctoral research project (02/12723-2). Portions of this work were performed at the Jet Propulsion Laboratory, California Institute of Technology, under contract with the National Aeronautics and Space Administration. The authors thank the referees for the constructive comments.

[45] Shadia Rifai Habbal thanks Paul R Gazis and another referee for their assistance in evaluating this paper.

References

Abraham-Shrauner, B., and S. H. Yun (1976), Interplanetary shocks seen by AMES plasma probe on Pioneer 6 and 7, *J. Geophys. Res.*, *81*, 2097.

Bai, T. (1990), Solar "hot spots" are still hot, *Astrophys. J.*, *364*, L17.

Berdichevsky, D. B., A. Szabo, R. P. Lepping, A. F. Viñas, and F. Mariani (2000), Interplanetary fast shocks and associated drivers observed through the 23rd solar minimum by Wind over its first 2.5 years, *J. Geophys. Res.*, *105*, 27,289.

Blanco-Cano, X., and S. Bravo (2001), Solar wind signatures associated with magnetic clouds, *J. Geophys. Res.*, *106*, 3691.

Bolton, S. J. (1990), One year variations in the near Earth solar wind ion density and bulk flow velocity, *Geophys. Res. Lett.*, *17*, 37.

Borrini, G., J. T. Gosling, S. J. Bame, and W. C. Feldman (1982), An analysis of shock wave disturbances observed at 1 AU from 1971 through 1978, *J. Geophys. Res.*, *87*, 4365.

Bothmer, V., and R. Schwenn (1998), The structure and origin of magnetic clouds in the solar wind, *Ann. Geophys.*, *16*, 1.

Bravo, S., and X. Blanco-Cano (1998), Signatures of interplanetary transients behind shocks and their associated near-surface solar activity, *Ann. Geophys.*, *16*, 359.

Bravo, S., and R. Pérez-Enriquez (1994), Coronal mass ejections associated with interplanetary shocks and their relation to coronal holes, *Rev. Mex. Astron. Astrofis.*, *28*, 17.

Cane, H. V. (1985), The evolution of interplanetary shocks, *J. Geophys. Res.*, *90*, 191.

Cane, H. V., N. R. Sheeley, and R. A. Howard (1987), Energetic interplanetary shocks, radio emission, and coronal mass ejections, *J. Geophys. Res.*, *92*, 9869.

Clúa de Gonzalez, A. L., V. M. Silbergleit, W. D. Gonzalez, and B. T. Tsurutani (2001), Annual variation of geomagnetic activity, *J. Atmos. Sol. Terr. Phys.*, *63*, 367.

Clúa de Gonzalez, A. L., V. M. Silbergleit, W. D. Gonzalez, and B. T. Tsurutani (2002), Irregularities in the semiannual variation of the geomagnetic activity, *Adv. Space Res.*, *30*, 2215.

Echer, E., and L. Svalgaard (2004), Asymmetry in the Rosenberg-Coleman effect around solar minimum revealed by wavelet analysis of the interplanetary magnetic field polarity data, *Geophys. Res. Lett.*, *31*, L12808, doi:10.1029/2004GL020228.

Echer, E., W. D. Gonzalez, L. E. A. Vieira, A. Dal Lago, F. L. Guarnieri, A. Prestes, A. L. C. Gonzalez, and N. J. Schuch (2003), Interplanetary shock parameters during solar activity maximum (2000) and minimum (1995–1996) 2003, *Braz. J. Phys.*, *33*, 115.

Echer, E., M. V. Alves, and W. D. Gonzalez (2004), Geoeffectiveness of interplanetary shocks during solar minimum (1995–1996) and solar maximum (2000), *Sol. Phys.*, *221*, 361–380.

Eselevich, V. G., and M. A. Filippov (1988), An investigation of the heliospheric current sheet (HCS) structure, *Planet. Space Sci.*, *36*, 105.

Fengui, W., and M. Dryer (1991), Propagation of solar flare-associated interplanetary shock waves in the heliospheric meridional plane, *Sol. Phys.*, *132*, 373.

Gazis, P. R. (1996), Solar cycle variation in the heliosphere, *Rev. Geophys.*, *34*, 379.

Gazis, P. R., J. D. Richardson, and K. I. Paularena (1995), Long term periodicity in solar wind velocity during the last three solar cycles, *Geophys. Res. Lett.*, *22*, 1165.

Gonzalez, W. D., B. T. Tsurutani, and A. L. Clúa de Gonzalez (1999), Interplanetary origin of geomagnetic storms, *Space Sci. Rev.*, *88*, 529.

Gosling, J. T. (1993), The solar flare myth, *J. Geophys. Res.*, *98*, 18,937–18,949.

Gosling, J. T., S. J. Bame, D. J. McComas, and J. L. Phillips (1990), Coronal mass ejections and large geomagnetic storms, *Geophys. Res. Lett.*, *17*, 901.

Hundhausen, A. J., S. J. Bame, and M. D. Montgomery (1971), Variations of solar-wind plasma properties: Vela observations of a possible heliographic latitude dependence, *J. Geophys. Res.*, *76*, 5145.

Kennel, C. F., J. P. Edmiston, and T. Hada (1985), A quarter century of collisionless shock research, in *Collisionless Shocks in the Heliosphere: A Tutorial Review*, *Geophys. Monogr. Ser.*, vol. 34, edited by R. G. Stone and B. T. Tsurutani, pp. 1–36, AGU, Washington, D. C.

Marsden, R. G., R. T. R. Sanderson, C. Tranquille, K. P. Wenzel, and E. J. Smith (1987), ISEE-3 observations of low-energy proton bidirectional events and their relation to isolated interplanetary magnetic structures, *J. Geophys. Res.*, *92*, 11,009.

Mendoza, B., and R. Pérez-Enriquez (1995), Geoeffectiveness of the heliospheric current sheet, *J. Geophys. Res.*, *100*, 7877.

Mihalov, J. D., C. T. Russel, W. C. Knudsen, and F. L. Scarf (1987), Pioneer Venus and near-Earth observations of interplanetary shocks, *J. Geophys. Res.*, *92*, 3385.

Neugebauer, M. (1975), Large-scale and solar-cycle variations in solar wind, *Space Sci. Rev.*, *17*, 221.

Neugebauer, M., and C. W. Snyder (1965), Solar-wind measurements near Venus, *J. Geophys. Res.*, *70*, 1587.

Newkirk, G., and L. A. Fisk (1985), Variation of cosmic-rays and solar-wind properties with respect to the heliospheric current sheet: 1.5 GeV protons and solar wind speed, *J. Geophys. Res.*, *90*, 3391.

Özgüç, A., T. Ataç, and J. Rybák (2002), Flare index variability in the ascending branch of solar cycle 23, *J. Geophys. Res.*, *107*(A7), 1146, doi:10.1029/2001JA009080.

Parks, G. K. (1991), *Physics of Space Plasmas, An Introduction*, 538 pp., Addison-Wesley, Boston, Mass.

Paularena, K. I., A. Szabo, and J. D. Richardson (1997), Coincident 1.3-year periodicities in the *ap* geomagnetic index and the solar wind, *Geophys. Res. Lett.*, *24*, 1435.

Priester, W., and D. Cattani (1962), On the semiannual variations of geomagnetic activity and its relations to the solar corpuscular radiation, *J. Atmos. Sci.*, *19*, 121.

Richardson, I. G., and H. V. Cane (1993), Signatures of shock drivers in the solar wind and their dependence on the solar source location, *J. Geophys. Res.*, *98*, 15,295–15,304.

Richardson, J. D., K. I. Paularena, J. W. Belcher, and A. J. Lazarus (1994), Solar wind oscillations with a 1.3 year period, *Geophys. Res. Lett.*, *21*, 1559.

Richter, A. K., K. C. Hsieh, H. Rosenbauer, and F. M. Neubauer (1986), Parallel fast-forward shock waves within 1 AU: Helios-1 and -2 observations, *Ann. Geophys.*, *4*, 1.

Rosenberg, R. L., and P. J. Coleman (1969), Heliographic latitude dependence of dominant polarity of interplanetary magnetic field, *J. Geophys. Res.*, *74*, 5611.

Russell, C. T., and R. L. McPherron (1973), Semiannual variation of geomagnetic activity, *J. Geophys. Res.*, *78*, 92.

Sawyer, C. (1974), Semiannual and solar-cycle variation of sector structure, *Geophys. Res. Lett.*, *1*, 295.

Schwenn, R. (1986), Relationship of coronal transients to interplanetary shocks: 3D aspects, *Space Sci. Rev.*, *44*, 139.

Sheeley, N. R., R. A. Howard, M. J. Koomen, D. J. Michels, R. Schwenn, K. H. Mühlhäuser, and H. Rosenbauer (1985), Coronal mass ejections and interplanetary shocks, *J. Geophys. Res.*, *90*, 163.

Smith, E. J. (2001), The heliospheric current sheet, *J. Geophys. Res.*, *106*, 15,819.

Sonnemann, G. R. (2002), Comment on 'Annual variation of geomagnetic activity' by Alicia L. Clúa de Gonzalez et al., *J. Atmos. Sol. Terr. Phys.*, *64*, 1667.

Szabo, A., R. P. Lepping, J. H. King, K. Paularena, and J. D. Richardson (1996), Twenty years of interplanetary magnetofluid variations with periods between 10 days and 3 years, in *Proceedings of Solar Wind 8*, edited by D. Winterhalter et al., p. 399, Am. Inst. Phys. Press, Dana Point, California.

Tsurutani, B. T., and R. P. Lin (1985), Acceleration of >47 keV ions and >2 keV electrons by interplanetary shocks at 1 AU, *J. Geophys. Res.*, *90*, 1.

Tsurutani, B. T., and X. Y. Zhou (2003), Interplanetary shock triggering of substorms: Wind and Polar, *Adv. Space Res.*, *31*, 1063.

Tsurutani, B. T., W. D. Gonzalez, F. Tang, and Y. T. Lee (1992), Great magnetic storms, *Geophys. Res. Lett.*, *19*, 73.

Volkmer, P. M., and F. M. Neubauer (1985), Statistical properties of fast magnetoacoustic shock wave in the solar wind between 0.3-AU and 1-AU– Helios-1,2 observations, *Ann. Geophys.*, *3*, 1.

Watari, S., and T. Detman (1998), In situ local shock speed and transit shock speed, *Ann. Geophys.*, *16*, 370.

Webb, D. F., and R. A. Howard (1994), The solar cycle variation of coronal mass ejections and the solar wind mass flux, *J. Geophys. Res.*, *99*, 4201.

Wilcox, J. M., and P. H. Scherrer (1972), Annual and solar magnetic cycle variations in interplanetary magnetic field, 1926–1971, *J. Geophys. Res.*, *77*, 5385.

Willis, D. M., P. R. Stevens, and S. R. Crothers (1997), Statistics of the largest geomagnetic storms per solar cycle (1984–1993), *Ann. Geophys.*, *15*, 719.

Winterhalter, D., E. J. Smith, M. E. Burton, N. Murphy, and D. J. McComas (1994), The heliospheric plasma sheet, *J. Geophys. Res.*, *99*, 6667.

Woo, R., and R. Schwenn (1991), Comparison of Doppler scintillation and in situ spacecraft plasma measurements of interplanetary disturbances, *J. Geophys. Res.*, *96*, 21,227.

Zhou, X., and B. T. Tsurutani (2001), Interplanetary shock effects on the nightside geomagnetic activity: Substorms, pseudobreakups, and quiescent events, *J. Geophys. Res.*, *106*, 18,957.

Zhou, X., and B. T. Tsurutani (2002), Interplanetary shock effects on the nightside auroral zone, magnetosphere and ionosphere, in *Space Weather Study Using Multipoint Techniques*, edited by L. Lyu, p. 139, Elsevier, New York.

Zieger, B., and K. Mursula (1998), Annual variation in near-Earth solar wind speed: Evidence for persistent north-south asymmetry related to solar magnetic polarity, *Geophys. Res. Lett.*, *25*, 841.

M. V. Alves, E. Echer, A. L. C. Gonzalez, W. D. Gonzalez, and L. E. A. Vieira, Geofísica Espacial, Instituto Nacional de Pesquisas Espaciais, Avenida dos Astronautas 1758, POB 515, São José dos Campos, SP, 12245-970, Brazil. (eecher@dge.inpe.br)

B. T. Tsurutani, Jet Propulsion Laboratory, California Institute of Technology, MS 169-506, 4800 Oak Grove Drive, Pasadena, CA 91109-8099, USA.